Direct Tunneling Current Model for Circuit Simulation

Chang-Hoon Choi, Kwang-Hoon Oh, Jung-Suk Goo, Zhiping Yu, and Robert W. Dutton

Center for Integrated Systems, Stanford University

Stanford, CA 94305-4075, USA

Abstract

This paper presents a compact direct tunneling current model for circuit simulation to predict ultra-thin gate oxide ($<$ 2.0 nm) CMOS circuit performance by introducing the explicit surface potential model and quantum-mechanical corrections. It demonstrates good agreements with the results from the numerical solver and measured data for the very-thin gate oxide thicknesses ranging 1.3 – 1.8 nm.

Introduction

According to the SIA roadmap, CMOS with gate length of 50–70 nm needs an oxide thickness of around 1.5–2.0 nm, which corresponds to 2–3 layers of silicon atoms. With such a thin oxide, direct tunneling occurs, resulting in exponentially increasing gate leakage current. This gate leakage current increases power dissipation and deteriorates device performance and circuit stability for ULSI [1]. However, even though there were many reports concerning the effects of the gate leakage current to MOS transistor operations, fewer studies have been made regarding impacts of the gate current to real circuit operations due to absence of a circuit simulation model for gate tunneling current. Hence, a gate tunneling current model is needed to observe circuit immunities depending upon circuit operations and circuit architectures against the gate leakage current. In this paper, a compact direct tunneling model for very-thin gate oxide MOS transistors suitable for circuit simulation is presented.

Surface potential based tunneling model

Fig. 1 shows direct tunneling of electrons across gate oxide from the p-type Si substrate to n^+-poly Si gate. This direct tunneling current model is expressed as [2],

$$J_{DT} = C(V_{ox}/t_{ox})^2 e^{\frac{-B(1-(1-V_{ox}/\Phi_B)^{3/2})}{V_{ox}/t_{ox}}} \quad (1)$$

where B and C are physical parameters (see [2]).

In order to use Eq. (1), it is necessary to relate the oxide voltage (V_{ox}) to the applied voltage (V_{gs}), since V_{ox} depends on V_{gs} as well as the surface potential (ψ_s) as:

$$V_{ox} = V_{gs} - V_{fb} - \psi_s \quad (2)$$

However, ψ_s can only be solved accurately using an iterative numerical approach, requiring expensive computation times, which is not desirable for circuit simulation. In order to reduce computation time while retaining accurate relations between the surface potential and the terminal voltages, an explicit formulation of surface potential (ψ_s) [3] is used in this work.

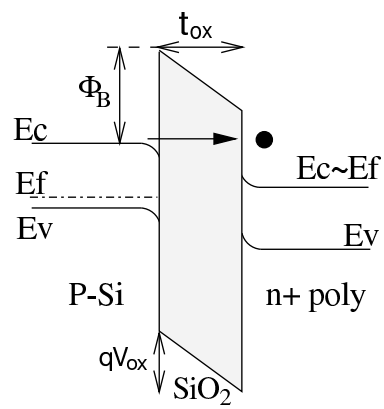

Fig. 1. Direct tunneling of electron in n^+-polysilicon / SiO_2 / p-Si MOS structure ($V_{ox} < \Phi_B$).

Under the assumption of the gradual channel approximation and the charge sheet approximation for an ideal n-type MOS transistor, the surface potential in the weak inversion region ($0 < \psi_s < 2\phi_f$) can be approximated as:

$$\psi_{s,weak} = V_{gb} - V_{fb} + \frac{\gamma^2}{2} - \gamma\sqrt{V_{gb} - V_{fb} + \frac{\gamma^2}{4}} \quad (3)$$

where γ is the body factor defined by $\sqrt{2q\epsilon_{Si}N_a}/C_{ox}$.

In the strong inversion region ($\psi_s > 2\phi_f$) ψ_s becomes

$$\psi_{s,strong} = 2\phi_f + V \quad (4)$$

where V denotes the electron quasi-Fermi potential, ranging from V_{sb} at the source and to V_{db} (= V_{ds} + V_{sb}) at the drain side. The surface potential at the drain node ($\psi_{s,drain}$) is modeled to consider the drain bias (V_{ds}) effect as,

$$\psi_{s,drain} = \psi_s(V_{ds} + V_{sb}), \quad \psi_{s,src} = \psi_s(V_{sb}) \quad (5)$$

This enables reduction of gate tunneling current at the drain as the drain bias increases due to the decrease of the potential difference between the gate and drain (i.e. decrease of V_{ox} at the drain). In addition, ΔV_{gs} is introduced to consider the channel length dependence on gate current related to the drain-induced barrier lowering (DIBL) effect as,

$$\Delta V_{gs} = \delta_{DIBL}\sqrt{2\phi_f + V_{sb}} \cdot V_{ds} \quad (6)$$

where $\delta_{DIBL} = \delta_O(\frac{L}{L_R})^{n_{dibl}}$, L_R is the reference gate length and n_{dibl} is an exponent of the length dependence. This ΔV_{gs} is added to V_{gb} in Eq. (3). As a result, effects of gate length

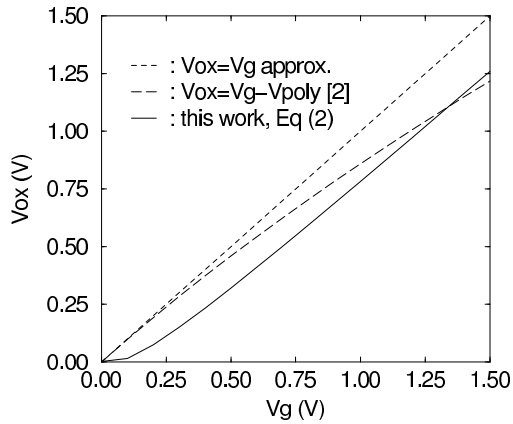

Fig. 2. Voltage drop at oxide (V_{ox}) with respect to the applied gate bias for t_{ox} = 1.5 nm. Comparisons between V_{ox} = V_g approximation, V_g - V_{poly}, and the surface potential based model.

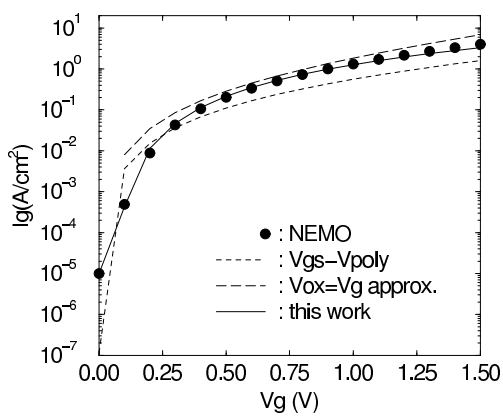

Fig. 3. Simulated gate current curves using V_g approximation, V_g - V_{poly}, and the surface potential based model, symbols are obtained from NEMO, an approximated Schrödinger equation solver (t_{ox} = 1.5 nm).

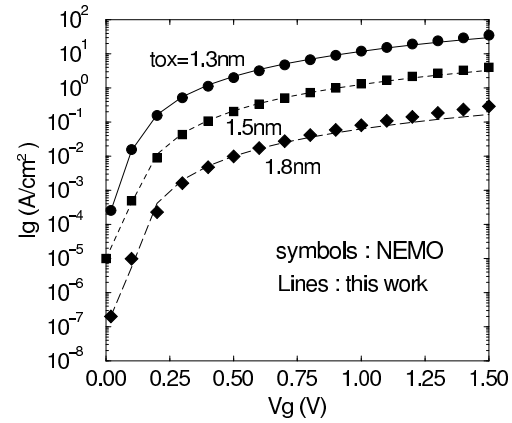

Fig. 4. Comparisons of simulated gate current using the compact model for different t_{ox}'s (1.3, 1.5, and 1.8 nm). Symbols denote gate current from NEMO.

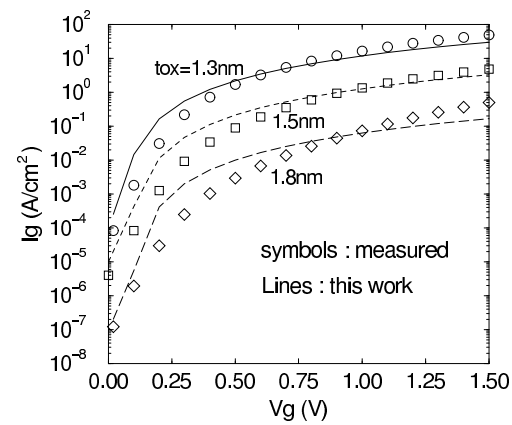

Fig. 5. Comparisons of simulated gate current using the compact model and measured data for different t_{ox}'s (1.3, 1.5, and 1.8 nm).

dependence of gate tunneling current is taken into account because ψ_s is abruptly increased as the channel length is scaled down.

Quantum-Mechanical effects

For gate oxide thicknesses less than 2.0 nm, quantum-mechanical effects become dominant. In the quantum-mechanical model, the inversion charge profile peaks at around 10 Å below the silicon surface such that inversion charge is effectively reduced to those of an equivalent oxide a few angstroms to nanometer thicker than the physical oxide. For an exact calculation of surface potential, an approximate manner by utilizing van Dort's bandgap broadening approach is used as [4],

$$\Delta E_g = \frac{\beta}{2kT} E_n^{2/3} \tag{7}$$

where E_n is the normal electric field at the Si-SiO_2 interface which is gate bias dependent determined by V_{ox} and t_{ox}, and β is a fact that can be determined experimentally. The value of ΔE_g is used to calculate a new intrinsic carrier concentration (n_i) and ϕ_f.

In the classical case, the electron density has its maximum value at the Si-SiO_2 interface, while in the quantum mechanical case the electron density is diminished at the interface, increases to its maximum value and decreases with the distance from the surface [5]. To model this, the surface electron concentration n_s in the inversion region is expressed as,

$$n_s = [1 - e^{-z_0^2/\lambda_{th}^2}] N_{sub} \cdot e^{(\psi_s - 2\phi_f)/kT} \tag{8}$$

where λ_{th} is the thermal wavelength as determined by the carrier effective mass with theoretical value of electron is 1.27 nm and z_0 is introduced for the finite concentration at the interface (z = 0).

Results and discussions

Fig. 2 shows the simulated oxide voltages (V_{ox}) with respect to gate bias using V_{ox} = V_g approximation, V_{ox} = V_g - V_{poly} [2], and the surface potential based model. Fig. 3 shows simulated gate currents using the compact model, the conventional methods [2][6] and 1D Green's function solver, NEMO [7], that is an approximated Schrödinger equation solver. Gate tunneling

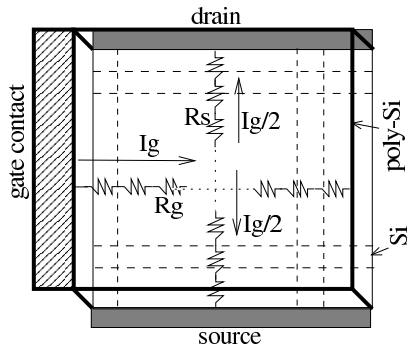

Fig. 6. Gate and series resistance (R_g and R_s) effects associated with gate current (I_g) in ultra-thin oxide, large area MOS transistor.

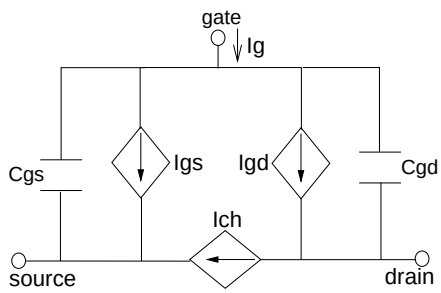

Fig. 7. Circuit model of gate tunneling current for circuit simulation (I_g = I_{gs} + I_{gd}).

current in the low gate bias obtained from the compact model agrees well with that from the numerical solver due to employing of the surface potential model in the weak inversion region. Comparing NEMO and real measurements, simulated gate currents for different oxide thicknesses are shown in Fig. 4 and 5. The simulated gate currents using the compact model agree well with those from NEMO for the oxide thicknesses of 1.3, 1.5, and 1.8 nm due to the considerations of the surface potential as well as quantum mechanical effects. The discrepancies between the measured and simulated data in Fig. 5 are probably caused by surface roughness, uncertainty in determining the effective oxide thickness, and the IR drop at the poly gate and

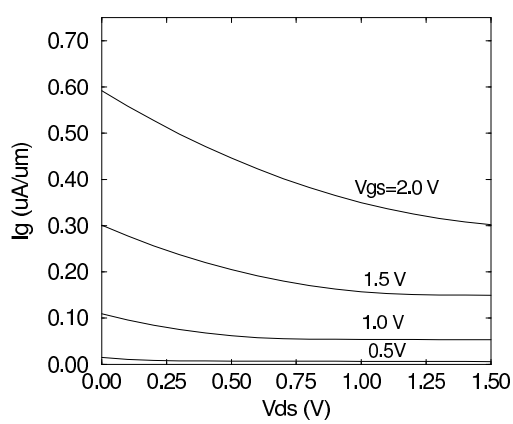

Fig. 8. Simulated gate tunneling current versus V_{ds} for different V_{gs}, t_{ox} = 1.5 nm.

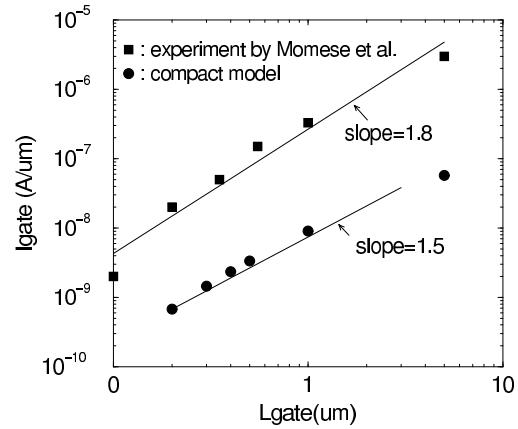

Fig. 9. Gate length dependence of gate tunneling current for t_{ox} = 1.5 nm, the simulated slope is comparable with ref. [7] due to consideration of DIBL.

the channel due to the gate leakage current. In reality, the gate tunneling current behavior in MOS terminals is affected by the three-dimensional geometric effects associated with gate (R_g) and series resistance (R_s), as shown in Fig. 6 [4].

In order to consider drain bias effects ($V_d > 0$ V) an equivalent circuit is used as in Fig. 7, where gate current (I_g) is composed of gate-to-source current (I_{gs}) and and gate-to-drain current (I_{gd}). Gate current in the drain (I_{gd}) is determined by surface potential at the drain ($\psi_{s,drain}$) for the given drain bias. Namely, I_{gs} and I_{gd} are computed independently by considering the surface potential of gate-to-source ($\psi_{s,src}$) and gate-to-drain ($\psi_{s,drain}$) in Eq. (5). In this work, these voltage-controlled current sources, I_{gs} and I_{gd}, were described by utilizing the behavioral modeling in SPICE, and BSIM3 model was used as a channel current (I_{ch}) model. As a result, as shown in Fig. 8 the simulated gate current decreases as the drain bias increases due to the increase of surface potential at the drain, which leads to V_{ox} reduction. The direction of gate current near the drain region can be even reversed when the potential of drain is higher than that of gate. Hence, total gate tunneling current becomes lower as the drain bias moves from the linear operation to the saturation regions; gate current effect is dominant at high V_{gs} and low V_{ds} bias conditions.

Fig. 9 illustrates the simulated channel-length dependence on gate current by consideration the DIBL effect; I_g decreases in inverse proportion to $L_g^{1.5}$, which is comparable the slope of the experiments (= 1.8) by Momose *et al* [8]. It is obvious that effects of gate tunneling current to the drain current become less problematic for the short channel lengths because the channel current is much higher than gate current and gate current decreases exponentially as the channel length is reduced. However, even though the gate current for individual transistor with very small size is not significant, the total gate current for the entire chip will become a serious problem for battery operations [9].

Fig. 10 (a) and (b) show the simulated drain currents for L_g = 20 μm and L_g = 50 μm when gate tunneling effects are considered. In long channel length (i.e. L_g = 50 μm) anomalous electric characteristics are appeared in very low V_d, because the

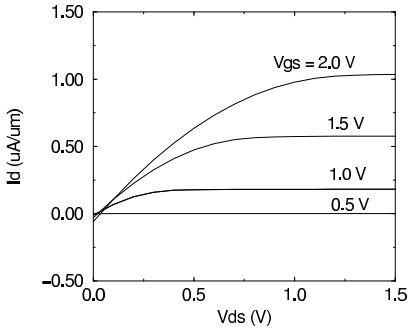

(a)

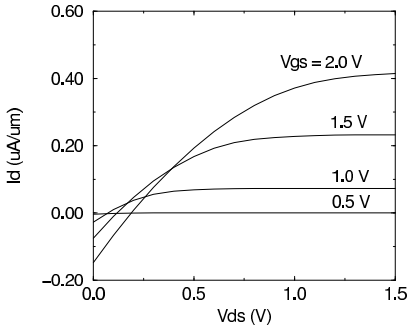

(b)

Fig. 10. Simulated drain current (I_d) versus V_d for t_{ox} = 1.5 nm, (a) L_g = 20 μm (b) L_g = 50 μm.

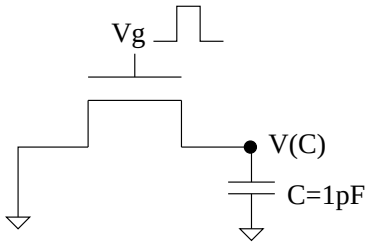

(a)

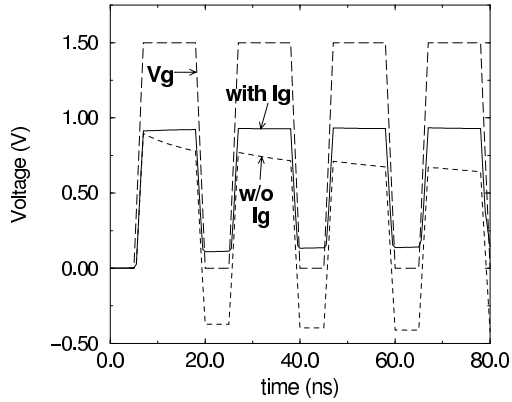

(b)

Fig. 11. Transient circuit simulation results with the gate current model, (a) W/L = 100 μm/100 μm, t_{ox} = 1.5 nm. (b) simulated $V(C)$ with and without gate tunneling models,

magnitude of gate current is comparable to the drain current in this bias range.

SPICE transient circuit simulation using the compact model is performed for the simple circuit as shown in Fig. 11, composed of a single NMOS transistor with a 1 pF capacitor. To observe the distinct effects of gate tunneling current during circuit operation, a large transistor (W/L = 100 μm/100 μm) is used in this case. With the compact model, gate tunneling current effect is remarkable; the voltage at the node of $V(C)$ keeps increasing even when gate bias is low.

Conclusions

An accurate direct tunneling model for circuit simulation is modeled by incorporation of the explicit surface potential model and quantum-mechanical corrections. The simulated gate current from this model demonstrates good agreements with the results from numerical solver and measured data for gate oxides ranging 1.3 – 1.8 nm.

Acknowledgment: The support from NSF through NCCE and DesCArtES projects is greatly appreciated.

References

[1] Y. Taur, D. A. Buchanan, W. Chen, D. J. Frank, K. E. Ismail, S. H. Lo, G. Sai-Halasz, R. Viswanathan, and *et al.*, "CMOS scaling into nanometer regime", *Proc. of the IEEE*, vol. 85, pp. 486–504, Apr. 1997.

[2] K.F. Schuegraf and C. Hu, "Hole Injection SiO_2 Breakdown Model for Very Low Voltage Lifetime Extrapolation," *IEEE Trans. Electron Devices*, vol. 41, pp. 761–767, 1994.

[3] R.van Langevelda, "A Compact MOSFET Model for Distortion Analysis in Analog Circuit Design," *PhD dissertation, Eindhoven Univ. of Tech.*, 1998.

[4] C.H. Choi, J.S. Goo, T. Y. Oh, Z. Yu, R. W. Dutton, A. Bayoumi, M. Cao, P. V. Voorde, and D. Vook, "C–V and Gate Tunneling Current Characterization of Ultra-Thin Gate Oxide MOS (t_{ox}=1.3–1.8 nm)", *in Proc. Symp. VLSI Technology*, pp. 151-152, 1999.

[5] N.D. Arora, *MOSFET Model for VLSI Circuit Simulation.* New York: Springer-Verlag, 1993.

[6] M. Depas, B. Vermeire, P.W. Mertens, R.L. Van Meirhaeghe, and M.M. Heyns, "Determination of Tunneling Parameters in Ultra-Thin Oxide Layer Poly-Si/SiO_2/Si Structures," *Solid-State Electron.*, vol. 38, pp. 1465–1471, 1995.

[7] C. Bowen, C. Fernando, G. Klimeck, A. Chatterjee, D. Blanks, R. Lake, J. Hu, J. Davis, M. Kulkarni, S. Hattangady and I-H Chen, "Physical oxide thickness extraction and verification using quantum mechanical simulation", *in IEDM Tech. Dig.*, pp. 869–872, 1997.

[8] H.S. Momose, M. Ono, T. Yoshitomo, T. Ohguro, S. Nakamura, M. Saito, and H. Iwai, "1.5 nm Direct-Tunneling Gate Oxide Si MOSFET's", *IEEE Tran. Electron Devices*, vol. 43, pp.1233–1242, Aug. 1996.

[9] H. Iwai and H.S. Momose, "Ultra-Thin Gate Oxides – Performance and Reliability," *in IEDM Tech. Dig.*, pp. 163–166, 1998.